Journal of Power Sources 251 (2014) 1–7

Contents lists available at ScienceDirect

Journal of Power Sources

journal homepage: www.elsevier.com/locate/jpowsour

Stability of carbon nanofibre-supported platinum catalysts in the presence of chloride under controlled mass-transfer conditions

Stein Trygve Briskeby [1], Mikhail Tsypkin, Reidar Tunold [2], Svein Sunde*

Department of Materials Science and Engineering, Norwegian University of Science and Technology (NTNU), NO-7491 Trondheim, Norway

HIGHLIGHTS

- Platinum catalysts were supported on carbon nanofibres.
- Chloride ions cause significant degradation during potential cycling.
- The main cause for the degradation is a decrease in the number of platinum particles.
- The degradation rate is dependent on the rotation rate.

ARTICLE INFO

Article history:
Received 20 July 2013
Received in revised form
8 October 2013
Accepted 24 October 2013
Available online 21 November 2013

Keywords:
Potential cycling
Platinum dissolution
Rotating disk
Re-deposition
Oxygen reduction reaction
Specific catalytic activity

ABSTRACT

The effect of chloride on the stability of platinum electrocatalysts was studied by rotating disk measurements in sulfuric acid electrolyte with a continuously increasing concentration of chloride anions. The activity towards oxygen reduction was found to be reduced by a factor of seven when 140 ppm chloride was present. Platinum corrosion was severe at high potentials, presumably accelerated by potential cycling, and greatly enhanced by mass transport. A five-fold increase in corrosion rate was found when the electrode was rotated at 1600 rpm with respect to stagnant conditions. At potentials where oxygen reduction occurs, dissolved Pt can be redeposited on the electrode. The Pt dissolution rate increased with increasing Cl^- concentration up to 20 ppm. Above this threshold the corrosion rate was unaffected by increases in Cl^- content.

1. Introduction

Polymer electrolyte membrane fuel cells (PEMFCs) are attractive low-emission power sources for electric propulsion vehicles [1]. When supplied with hydrogen produced from renewable energy sources such as wind or solar energy, they have the potential of producing electricity without other emissions than water. Although the technology has come far, and automobile manufacturers and fuel cell developers have produced PEMFC vehicles for years, two major challenges remain: cost and lifetime [2].

Several factors can reduce the lifetime of the fuel cell, including platinum-particle dissolution and agglomeration, carbon support corrosion and membrane thinning. Additionally impurities, either from fuel or air can accelerate degradation. Typical fuel impurities include CO, CO_2, NH_3 and H_2S originating from reforming of hydrocarbons. NH_3 and H_2S are critical impurities, as irreversible degradation occurs [2]. Traces of ammonia can be formed in natural gas-reforming processes, and levels as low as 10 ppm can seriously impact the performance [3]. Long-term exposure can give irreversible reduction in performance. Impurities originating from air supply to the cathode can be SO_2, NO_2, H_2S and NO, and have been reported to give irreversible damage to PEMFC [4–7].

Anionic impurities can be introduced to the membrane electrode assemblies (MEA) from water-cooling systems/humidifiers or as residual from catalyst production. When fuel cells are used in road transportation, saline air or de-icing of roads may be an anion source [2]. Matsuoka et al. [8] investigated the impact of Cl^-, F^-, SO_4^{2-} and NO_3^- on fuel cell performance. It was found that only chloride had a negative effect on the fuel cell voltage during operation. A platinum loss of 30% after 50 h operation was reported.

* Corresponding author. Tel.: +47 735 94051; fax: +47 73 59 11 05.
E-mail address: Svein.Sunde@material.ntnu.no (S. Sunde).
[1] Current address: Statoil ASA, Herøya Forskningspark, Hydroveien 67, Norway.
[2] 1933–2013.

0378-7753/$ – see front matter © 2013 Elsevier B.V. All rights reserved.
http://dx.doi.org/10.1016/j.jpowsour.2013.10.148

Several authors have shown increased degradation rates of fuel cell electrocatalysts in the presence of chloride impurities. Mitsushima et al. [9] studied the solubility of Pt in different electrolytes. They found a much higher concentration of dissolved Pt when Cl^- was added. A linear dependency on the Cl^- concentration up to 2.8 mM was found. The increased solubility was attributed to the presence of chloride complexes. In the work of Yadav et al. [10], the effect of Cl^- on electrodeposited Pt was studied with an electrochemical quartz crystal microbalance (EQCM). The loss of Pt was suggested to by caused by the following reactions [11,12]:

$$Pt + 4Cl^- \rightarrow PtCl_4^{2-} + 2e^- \quad (1)$$

$$Pt + 6Cl^- \rightarrow PtCl_6^{2-} + 4e^- \quad (2)$$

The degradation appeared to be relatively insignificant below 100 ppm. However, for nanosized Pt particles the corrosion rate can be significant, as was shown by our electrochemical quartz crystal microbalance (EQCM) [13] in which an electrode made from a fuel cell catalyst (50 wt.% Pt/C) lost 10% of its platinum content over a 24 h period when exposed to a sulfuric acid solution containing 10 ppm of chloride and at a constant potential of 1.2 V vs. a reversible hydrogen electrode (RHE). Li et al. [14] investigated the effects of trace amounts of chlorine in PEM fuel cells to address the possibility of using hydrogen from the chlor-alkali industry as a fuel in PEM fuel cells. In line with our results [13], Li et al. [14] also found a significant, non-recoverable loss in electrochemical surface area (ECSA). This group later investigated the loss of ECSA in catalysts of fuel cell catalysts (46 wt.%) by the use of EQCM and found losses of 4%, 7% and 13% during 1000 potential cycles at a rate of 50 mV s^{-1} from 0.4 V to 1.2 V in 500, 1000, and 2000 ppm, respectively [15]. The duration of these experiments is therefore much shorter than those in Ref. [13], and a direct comparison is difficult. However, the almost instantaneous 50% loss even at 50 ppm in Ref. [13] would seem to indicate that chloride is more aggressive during potentiostatic hold than during cycling. Later results in a PEM fuel cell appears to indicate that also the mass transfer is affected by chloride contaminations [16]. A related result was found by Baturina et al. [17], who found that the presence of HCl during fuel cell operation influenced also the part of the polarization curve dominated by the diffusion of molecular oxygen. The effect of mass transport on degradation rate, on the other hand, is to our knowledge not yet reported.

The presence of chloride may also affect rates of the fuel cell reactions themselves. Schmidt et al. [18] studied the oxygen reduction reaction on a carbon supported Pt fuel cell catalyst in the presence of different anions and found that the oxygen reduction reaction (ORR) activity decreased in the order $ClO_4^- > HSO_4^- > Cl^-$. The results were similar to those for smooth polycrystalline and single crystal Pt electrodes, and consistent with the increasing adsorption bond strength of the anions. Enhanced formation of H_2O_2 in the presence of Cl^- was also encountered in these experiments, and the need for chloride free electrode preparation schemes in order to avoid performance losses and/or corrosion/degradation effects was stressed. Similar results were reported by Baturina et al. [17].

Replacing the classical carbon-black supports such as Vulcan XC-72, may influence the catalytic activity significantly [19–23]. For example, we recently showed that there is a significant gain in terms of the activity for the methanol oxidation reaction if XC-72 is replaced by carbon nanofibers [24]. It therefore becomes of significance to investigate the stability of catalyst deposited on such supports with relevant impurities present in the fuel.

Below we present results demonstrating the effect of mass transfer on Pt-dissolution and the oxygen-reduction reaction at a carbon nanofibre-supported Pt catalyst for PEM fuel cells. For our studies we employed a controlled, continuous release of Cl^- from a Saturated Calomel Electrode (SCE) reference electrode to quantify the influence of Cl^- on the Pt corrosion. We thus also show how to extract data for chloride-induced dissolution of Pt under continuously changing concentrations of the chloride, which may be methodologically useful in corrosion studies of PEM fuel cell catalysts.

2. Experimental

A modified polyol method [25,26] was used for preparation of a 10 wt.% Pt catalyst on platelet carbon nanofibre support. 200 mg of carbon was dispersed in 50 ml of ethylene glycol (VWR, AnalaR NORMAPUR™). The suspension was ultrasonicated for 30 min. After the ultrasonic treatment, 50 ml of a precursor solution (H_2PtCl_6 (VWR) in ethylene glycol) corresponding to 10 wt.% nominal loading and 0.4 g of NaOH (Alfa Aesar p.a) was added. The mixture was heated and kept at 160 °C for 1/2 h under Ar atmosphere before cooling to room temperature. 100 ml of de-ionized water was added and the sample allowed to settle to sedimentation for 6 h. The resulting catalyst was filtered and washed thoroughly with de-ionized water and dried.

Thin film electrodes were prepared by a procedure described by Schmidt et al. [27] and Paulus et al. [28]. In short, 20 μl of a slurry containing 1 mg catalyst per 1 ml of a 20% isopropanol in water solution was pipetted on to the disk of a rotating ring-disk electrode (RRDE, Pine). After drying under Ar, 20 μl of a Nafion solution (Alfa Aesar 5% w/w) diluted 1:100 with water was applied to the electrode, forming a thin Nafion film after water evaporation.

Electrochemical experiments were performed in a three electrode setup using an SCE (Pine Instruments) or a Reversible Hydrogen Electrode (RHE) as reference electrode placed directly into the solution. However, all potentials are reported vs. RHE. A Pt wire enclosed in a separate compartment with a glass sinter separator was used as counter electrode, except for the measurements involving ICP for which a Pd wire was employed. All measurements were conducted in a 0.5 M H_2SO_4 (Merck, p. a.) electrolyte saturated with oxygen (AGA, 5.0). All glassware in contact with the electrolyte was carefully cleaned by boiling in a solution of 71 vol. % de-ionized water, 28 vol. % H_2O_2 (35%) and 1 vol. % concentrated H_2SO_4 in order to remove organic impurities.

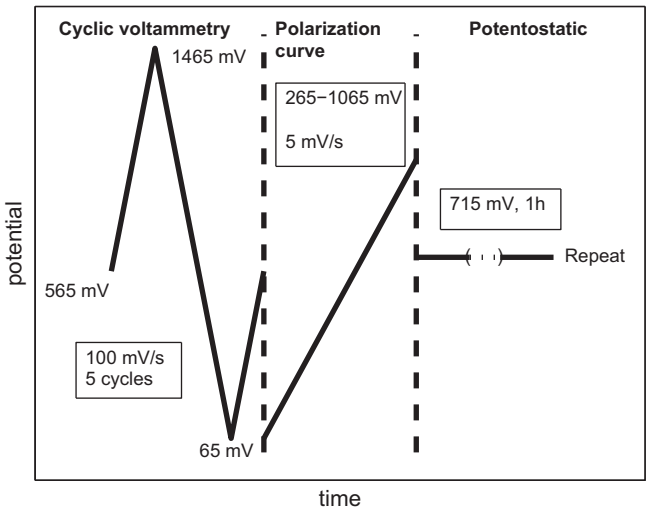

Fig. 1. Electrochemical test procedure.

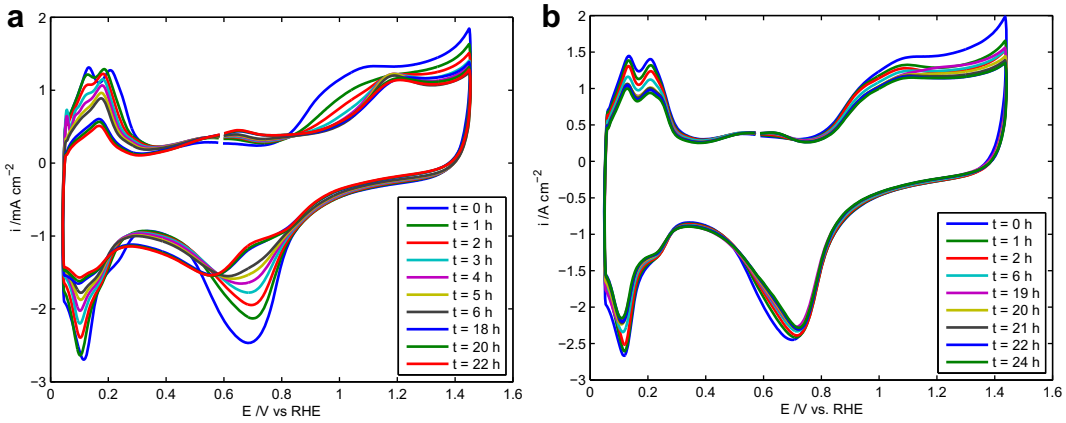

Fig. 2. Cyclic voltammograms recorded over 24 h of degradation tests. (a) shows experiments in a cell with an SCE electrode, and (b) shows the results in a cell with an RHE reference electrode. The times at which the voltammograms were recorded is given in the legend in hours.

The glassware was thoroughly rinsed with water to remove the cleaning solution before experiments started.

The electrochemical measurement sequence is depicted in Fig. 1. The sequence was repeated continuously over the course of the experiments. However, the length of the potentiostatic holds was varied. One sequence contained 5 voltammetric cycles with a sweep rate of 100 mV s^{-1}. The start and stop potential was 565 mV. Upper and lower vertex potentials were 1465 mV and 65 mV respectively. Following the cyclic voltammetry, a polarization curve was recorded between 265 mV and 1065 mV at a sweep rate of 5 mV s^{-1}, before a potentiostatic hold at 715 mV for 1 h. During the recording of the polarization curve and the potentiostatic hold, the electrode was rotated at 1600 rpm. Measurement series were performed both with and without rotation during cyclic voltammetry.

Samples of the electrolyte were analyzed with Inductively Coupled Plasma (ICP) to measure the content of dissolved Pt and transport of K^+ from the SCE reference electrode to the electrolyte.

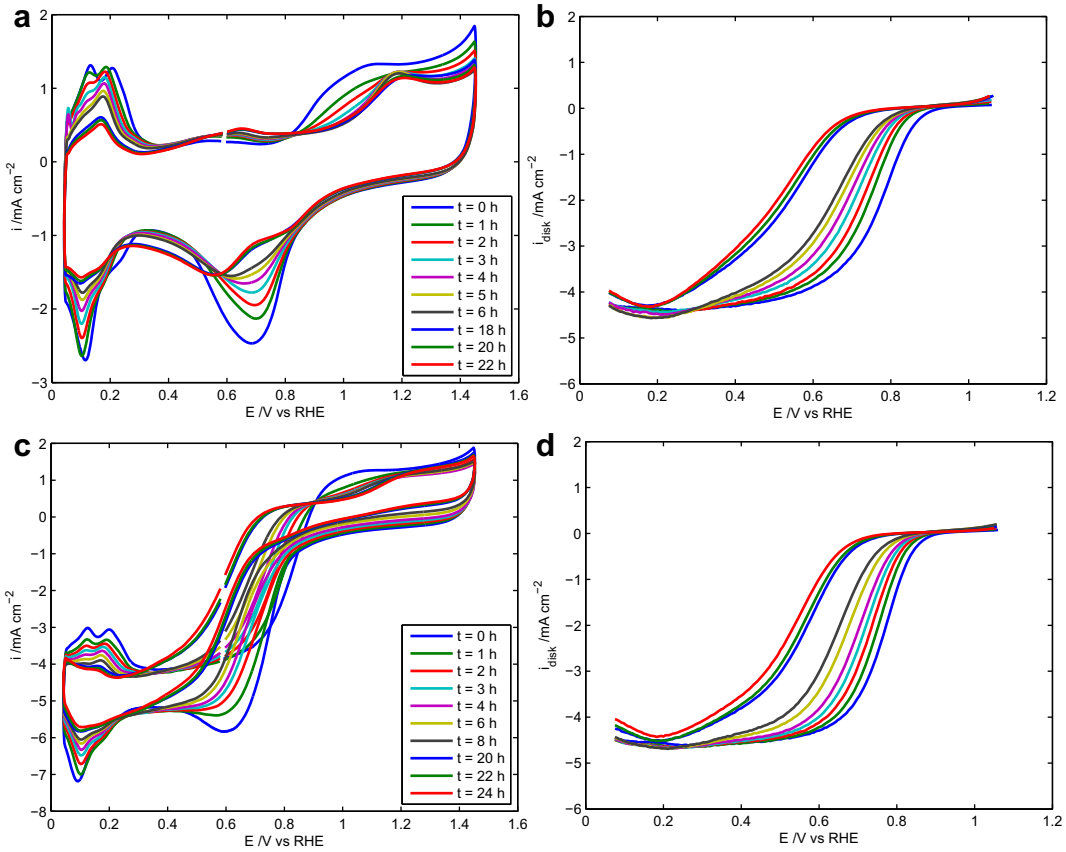

Fig. 3. Cyclic voltammograms (a) and polarization curves (b) from measurement series without rotation of the electrode during cyclic voltammetry. Cyclic voltammograms (c) and polarization curves (d) from measurement series with rotation of the electrode during cyclic voltammetry. All measurements are recorded using a saturated calomel reference electrode (SCE). The Cl^- content in the electrolyte is increasing by time according to Fig. 7(b) due to a constant leakage of ions from the reference electrode.

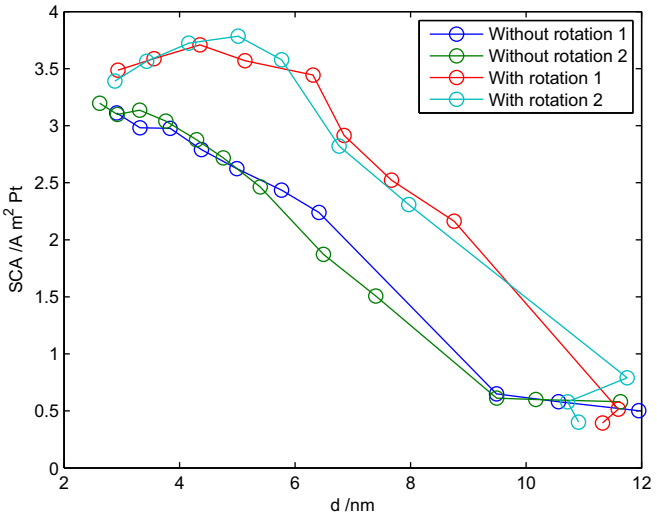

Fig. 4. Specific catalytic activity (SCA) as a function of Pt particle size. The concentration of Cl^- is increasing according to Fig. 7(b) moving from left to right in the plot.

Ion chromatography was used to analyze the Cl^- content of the electrolyte. Aliquots for analysis were sampled from the electrolyte after each series of cyclic voltammetry and linear polarization.

Transmission Electron Microscopy (TEM) images were recorded of catalyst samples that were electrochemically degraded by means of a JEOL 2010F electron microscope equipped with a field emission gun. TEM samples were prepared by dispersing the used catalyst in water and placing one droplet of dispersion on a holey carbon TEM grid.

3. Results and discussion

Fig. 2 shows cyclic voltammograms of the carbon nanofibre-supported Pt catalyst in a cell with an SCE reference electrode (a), and in a cell with an RHE reference electrode (b). In the cell with the SCE the platinum oxide region in the voltammogram is suppressed and shifted towards higher potentials, and there is a negative potential shift in the hydrogen underpotential deposition (UPD) peaks. In the cell with the RHE, no such effects are apparent.

As will be demonstrated below, the SCE electrode caused a steady supply of Cl^- ions to the electrolyte. In other words, the results in Fig. 2 correspond to solutions with (a) and without (b) a continuous supply of Cl^-. The effect of adding chloride can be clearly seen. In Fig. 3(a) where the concentration of Cl^- is continuously increasing, strong adsorption of chloride appears as a suppression of, and shift towards higher potential of the platinum oxide region in the voltammogram, and a negative potential shift in the hydrogen underpotential deposition (UPD) peaks. Similar effects on the voltammogram shape is also reported by ourselves and others [13,29,15]. In the chloride-free system (Fig. 2(b)) on the other hand, the shape of the voltammogram remains virtually unchanged

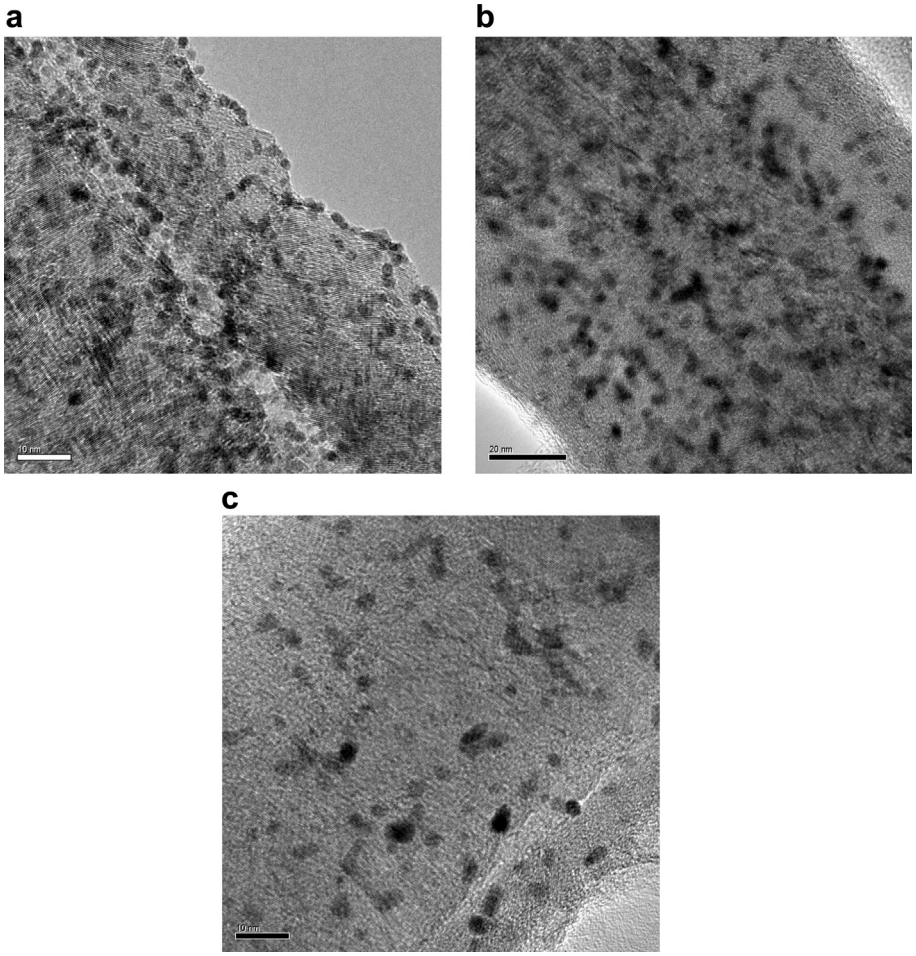

Fig. 5. TEM micrographs of (a) initial catalyst, (b) after 4 h degradation (~30 ppm Cl^-), (c) at the end of the test, 24 h (~140 ppm Cl^-). The electrode was not rotated during cyclic voltammetry measurements, and the chloride concentration increased linearly with time.

over the course of the experiments, except for a reduction in active surface area visible as lowering in peak heights.

Fig. 3 shows cyclic voltammograms and polarization curves recorded at rotating disk electrodes (RDE), with and without electrode rotation. The UPD charge from the hydrogen region of the cyclic voltammograms (Fig. 3(a) and (c)) was used to calculate the ECSA over time. The ECSA was, in turn, used to calculate the specific catalytic activity (SCA in A m^{-2} Pt) from the oxygen reduction current recorded during linear scan voltammetry (RDE measurements in Fig. 3(b) and (d)).

Fig. 4 shows the resulting SCA as a function of Pt particle size calculated from hydrogen UPD assuming spherical monodisperse particles.[3] Four data series are displayed, two for which the electrode was rotated (at 1600 rpm) and two for which it was not. (The abscissa axis can thus also be understood as representing time.) The potential was held at 715 mV vs. RHE, which is in the region of mixed reaction control. As is seen from Fig. 4, activity dropped by a factor of seven from the initial activity at the end of the experiment in both cases. However, in the experiments where the electrode was rotated during the cyclic voltammetry, an apparent increase in SCA was observed during the first hours of the experiments.

We ascribe part of the drop in activity in Fig. 4 to strong adsorption of chloride on Pt hindering the adsorption of oxygen, and thus shifting the reduction wave in the polarization curves in Fig. 3 to lower potentials [18,29].

The difference in the behavior with and without rotation cannot be easily explained by adsorption of chloride and is likely to be related to Pt dissolution. Since the data were normalized with respect to surface Pt area, this implies that the specific electrocatalytic properties change during the dissolution. Changes like those in the figure may be due to the structure of the catalyst particles (development of steps, edges, and facets [30–32]), size effects [33–35], or the average distance between the catalyst particles [36] developing differently during the dissolution–redeposition process. (We attempted to take particle size effects explicitly into account in Fig. 4. However, due to dissolution the particle size changes much less than what it appears to from the figure, see below.)

Fig. 5 presents TEM images of the pristine catalysts, of a catalyst collected after 4 h, and of a catalyst collected after 24 h. Fig. 6 shows corresponding size histograms collected from Fig. 5. After 4 h some particle growth is apparent, and the distribution is wider. After 24 h, the initial growth stopped, and the distribution is essentially the same as that after 4 h. Also, a considerable amount of Pt was lost, Fig. 5(c). The particle growth is of similar magnitude, though, or perhaps a little less than that found by Baturina et al. [17] for a cathode catalyst in a fuel cell exposed to HCl, who also observed a broadening in the size distribution.

The actual change in the particle size is thus presumably grossly exaggerated by the calculation of particle size in Fig. 4, but the distance between them obviously increases. In view of this an explanation within the territory of Watanabe et al. [36] is possible. This theory contends that if the support is active in transporting reactants and products of the electrochemical reaction the interparticle distance may affect the overall rate of the electrochemical reaction. In a more recent study Yang et al. [37] suggested that increasing interparticle distance increases the degree to which oxygen is reduced to H_2O_2 rather than H_2O due to lower rates of readsorption of reaction intermediates and thus the apparent ORR current.

[3] Dissolution of Pt is not included in these calculations. Calculations including this would lead to smaller particle sizes at longer times.

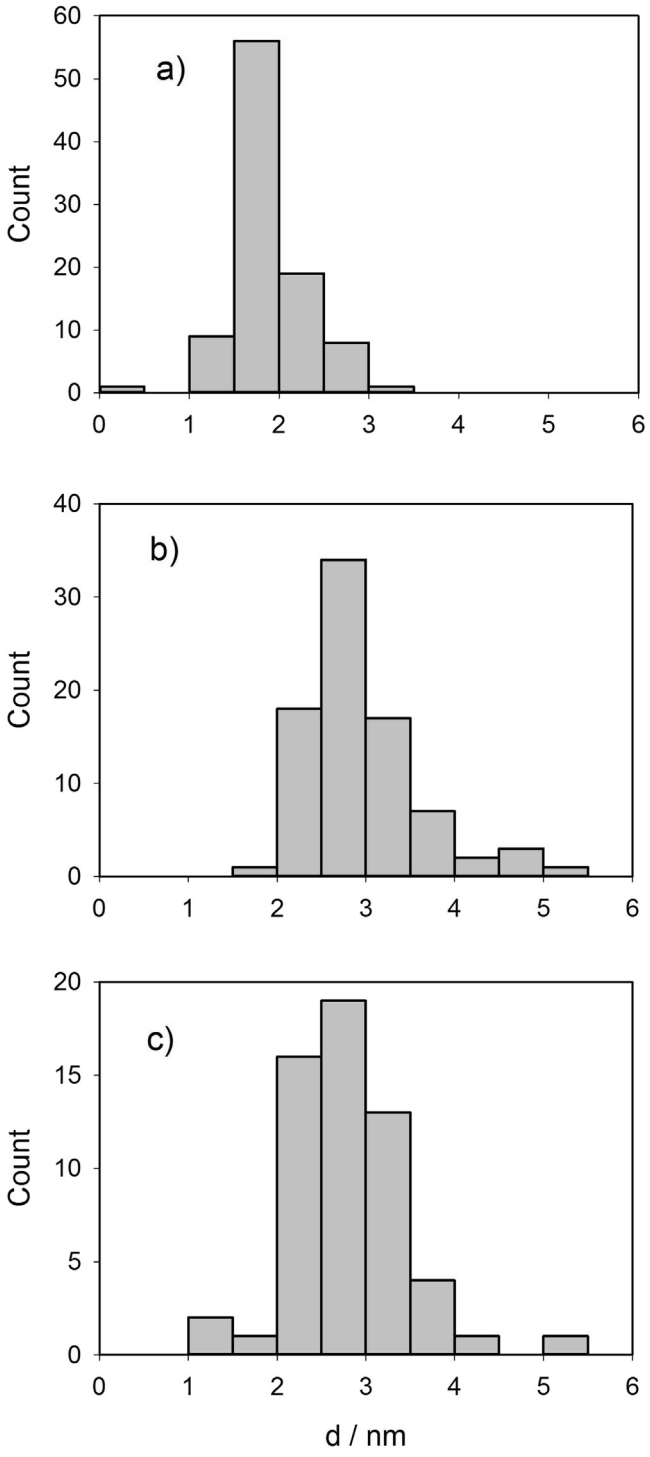

Fig. 6. Histograms for the TEM images in Fig. 5. The labels of the histograms are the same as the corresponding TEM images in Fig. 5.

The rate of Pt dissolution will in general depend on the rates of reactions (1) and (2), and on the rates of these reactions in reverse (re-deposition). The standard redox potential of $PtCl_6^{2-}$ to $PtCl_4^{2-}$ is 1.09 V and that for reduction of $PtCl_4^{2-}$ to Pt is 0.93 V vs. RHE [38]. At potentiostatic holds at 715 mV we thus expect redeposition (for similar activities of $PtCl_4^{2-}/PtCl_6^{2-}$ and Cl^-) of Pt species dissolved at high potentials during cycling. The net rate of dissolution of Pt will therefore be dependent on flow conditions

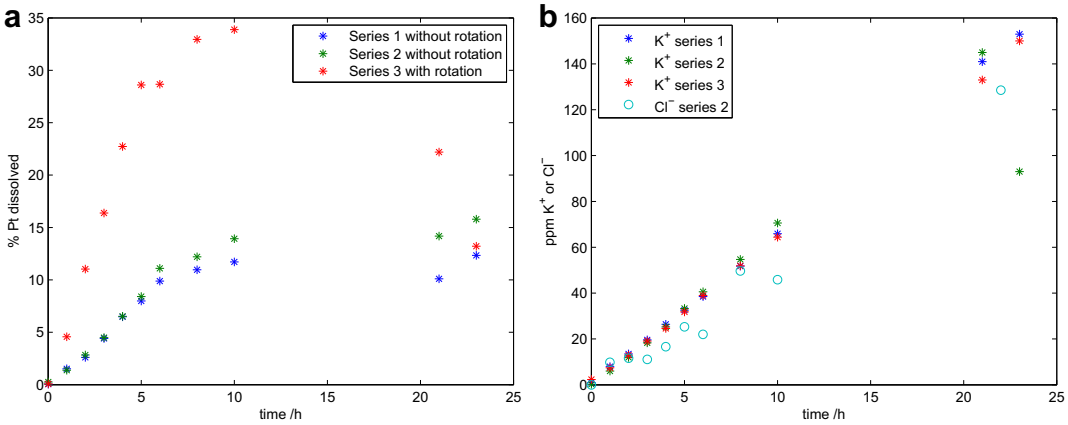

Fig. 7. Amount of Pt dissolved from the electrode (a) and K^+ and Cl^- concentrations as a function of time (b).

(rotation) both through transport of Cl^- to the electrode and Pt species away from the electrode.

Fig. 7(a) and (b) shows the calculated Pt loss based on ICP measurements and the accumulated concentrations of K^+ and Cl^- respectively. As can be seen there is a steady increase in the concentration of Cl^- and K^+ in the electrolyte caused by leakage of KCl from the reference electrode. The chloride concentration c_{Cl^-} reached a level of 140 ppm over 24 h. The dissolution of Pt is known to accelerate in the presence of Cl^- due to strong chloride adsorption causing a positive shift in the potential for Pt–OH formation. The delayed growth of a protective oxide layer facilitates the formation of soluble chloride complexes when Pt is oxidized [13,29]. The results of Fig. 7 are in line with these facts.

In Fig. 7 the Pt concentration levels off after some 5 h, or is even reduced at longer times. Between $t = 10$ h and 20 h the electrode was held at constant potential (715 mV vs. RHE). Therefore, this indicates that Pt either redeposits at the working electrode or, alternatively, that negatively charged Pt complexes like $PtCl_6^{2-}$ to $PtCl_4^{2-}$ migrate to the positive counter electrode.

At short times ($t < 5$ h), due to the low concentration of dissolved Pt the influence of redeposition is expected to be small. Fig. 8(a) shows the experimental data for the first data points before the leveling off of the Pt concentration (c.f. Fig. 7(a)). The data points were fitted to a third-order polynomial which was further differentiated to find the Pt dissolution rate. In Fig. 8(b), the rate of Pt dissolution vs. the concentration of Cl^- is plotted. (The Cl^- concentration is assumed to be equal to the measured K^+ concentration, since chloride data was not available for all data series. As seen from Fig. 7 this approximation is reasonable, and the additional source of error introduced in the calculations appears to be small.) The rate of platinum dissolution as a function of the chloride concentration at a time t_1 ($r(C_{Cl^-}(t_1))$) can be found from the slope of the curve by assuming that the reaction rate is given by

$$C_{Pt}(t_1) = \int_0^{t_1} r(C_{Cl^-}(t))\mathrm{d}t \tag{3}$$

and thus

$$r(C_{Cl^-}(t_1)) = \frac{\mathrm{d}C_{Pt}}{\mathrm{d}t_1} \tag{4}$$

Here C_{Pt} and C_{Cl^-} are the concentrations of Pt and Cl^-, and t is time. (We assume that the effect of the bulk platinum concentration on the net dissolution rate through re-deposition can be safely neglected in Equations (3) and (4) since the concentration of Pt in solution are orders of magnitude lower than that of chloride at all times during the experiment.)

As seen from Fig. 8(b) the initial slope is similar for the two data series without rotation. A higher slope is observed in the third series with rotation. This is expected as mass transport to the electrode is enhanced by convection. At higher chloride concentrations a flattening is observed in two of the curves. This can be understood by looking at the voltammograms in Fig. 3. It is seen that increasing the Cl^- concentration has more influence on the

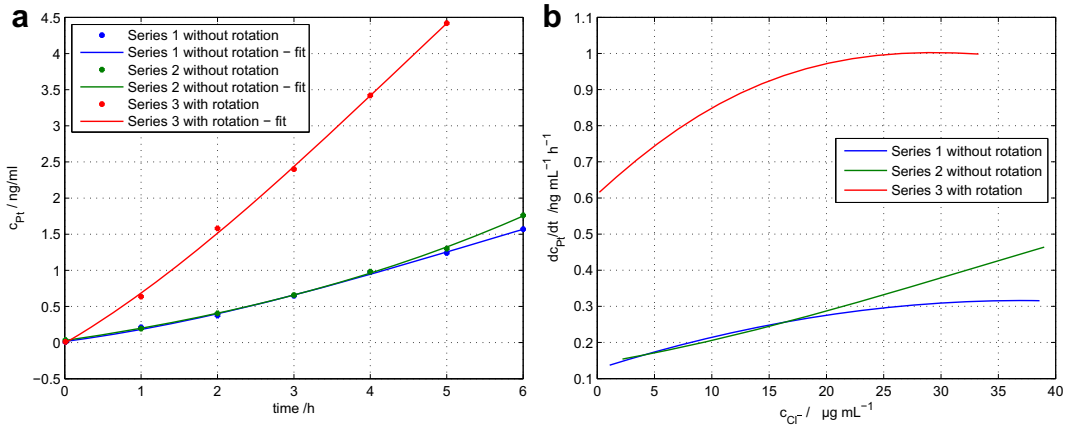

Fig. 8. (a) Measured concentration of dissolved Pt in the electrolyte for the first 6 h of experiment. Solid lines are the corresponding third degree polynomial fits. (b) Pt dissolution rate as function of Cl^- concentration calculated as the derivative of the polynomials in (a).

shape of the voltammograms at low Cl^- concentrations than in the high concentration range. After 4 h the shape of the voltammograms in the Pt-oxide region has ceased to change, which could imply that the Pt surface has a saturation coverage of Cl^-. Thus, above this limit, further increase in Cl^- would not result in increased dissolution rates, after which dissolution is a function of number of cycles, and the lines in Fig. 8(b) should become straight with zero slope. As we pointed out in Ref. [13] in our work on studying platinum dissolution in presence of chloride by EQCM, no change in the shape of the voltammogram was seen above 20 ppm Cl^-. The data presented here are in the same range.

The highest measured Pt concentration in the electrolyte was found when the electrode was rotated, and corresponded to dissolution of close to 35% of the total Pt mass on the electrode. With a stagnant electrode, a 15% loss was recorded. This loss is realistic when consulting the data of Ofstad et al. [13], in which a 25% loss was found over a 7 h potentiostatic hold at 1.2 V. Our results here, however, indicate that cycling has higher impact on catalyst stability than potentiostatic holds in the oxide region, as the total time at potentials above 1.2 V in our case is less than 3 min over 6 h experiments. The accelerated dissolution is likely to be enhanced by restructuring of the Pt surface caused by formation of oxide followed by oxide reduction during cycling [29].

We emphasize that the measurements here are comparable with our previous results for similar catalysts employing an RHE reference electrode and with chloride added directly to the electrolyte under stagnant conditions. For example, with 10 ppm in the solution the mass loss rate in Ref. [13] was some 0.5% per hour, increasing to an average of approximately 2% at 10 ppm. By comparing Figs. 7 and 8 we find that at 10 ppm the mass loss rate is approximately 1% per hour and increasing by a factor of 2 when the chloride concentration doubles. In view of the uncertainties displayed in Fig. 8 we consider this a relatively good agreement.

This work confirms that corrosion of Pt can be auto-inhibited by chloride at high concentrations meaning that the reaction rate for platinum dissolution increases with increasing Cl^- concentration at low Cl^- concentrations reaching a plateau as chloride content increases. Mass transport is seen to have a significant impact on corrosion. A five-fold increase in corrosion rate was seen when the electrode was rotated at 1600 rpm. The different concentration gradient and possibility for redeposition in the case of a stagnant electrode are believed to be the cause.

4. Conclusion

The activity towards oxygen reduction was found to be reduced by a factor of seven when chloride was present at concentrations up to 140 ppm. Platinum corrosion is severe at high potential, presumably accelerated by potential cycling. Pt dissolution is greatly enhanced by increasing mass transport. A five-fold increase is seen when the electrode is rotated at 1600 rpm. Over time, a flattening in the concentration of dissolved Pt was observed, which can partly be explained by redeposition of Pt at oxygen reduction potentials. The Pt dissolution rate increases with increasing Cl^- concentration up to 20 ppm. Above this threshold the corrosion rate is unaffected by increases in the Cl^- content.

Acknowledgments

Work at NTNU was supported by The Norwegian Research Council through the NANOMAT program, contract no 158516/S10 and the EU project FURIM (6th EU Framework Programme, contract no. SES6-CT-2004-502782). John Walmsley from SINTEF, Materials and Chemistry is acknowledged for assistance with TEM data collection.

References

[1] P. Costamagna, S. Srinivasan, J. Power Sources 102 (2001) 253–269.
[2] R. Borup, J. Meyers, B. Pivovar, Y.S. Kim, R. Mukundan, N. Garland, D. Myers, M. Wilson, F. Garzon, D. Wood, P. Zelenay, K. More, K. Stroh, T. Zawodzinski, J. Boncella, J.E. McGrath, M. Inaba, K. Miyatake, M. Hori, K. Ota, Z. Ogumi, S. Miyata, A. Nishikata, Z. Siroma, Y. Uchimoto, K. Yasuda, K.-i. Kimijima, N. Iwashita, Chem. Rev. 107 (2007) 3904–3951.
[3] R. Halseid, P.J. Vie, R. Tunold, J. Power Sources 154 (2006) 343–350.
[4] Y. Nagahara, S. Sugawara, K. Shinohara, J. Power Sources 182 (2008) 422–428.
[5] W. Schmittinger, A. Vahidi, J. Power Sources 180 (2008) 1–14.
[6] A.J. Steinbach, C.V. H Jr., M.K. Debe, ECS Trans. 11 (2007) 889–902.
[7] R. Mohtadi, W.k. Lee, J.V. Zee, J. Power Sources 138 (2004) 216–225.
[8] K. Matsuoka, S. Sakamoto, K. Nakato, A. Hamada, Y. Itoh, J. Power Sources 179 (2008) 560–565.
[9] S. Mitsushima, Y. Koizumi, S. Uzuka, K.-I. Ota, Electrochim. Acta 54 (2008) 455–460.
[10] A. Yadav, A. Nishikata, T. Tsuru, Electrochim. Acta 52 (2007) 7444–7452.
[11] D. Johnson, D. Napp, S. Bruckenstein, Electrochim. Acta 15 (1970) 1493–1509.
[12] O. Ginstrup, I. Leden, Acta Chem. Scand. (1947–1999) 22 (1968) 1163.
[13] A.B. Ofstad, M.S. Thomassen, J.L.G. de la Fuente, F. Seland, S. Møller-Holst, S. Sunde, J. Electrochem. Soc. 157 (2010) B621–B627.
[14] H. Li, H. Wanga, W. Qiana, S. Zhanga, S. Wessel, T.T. Cheng, J. Shena, S. Wu, J. Power Sources 196 (2011) 6249–6255.
[15] A. Lam, H. Li, S. Zhang, H. Wang, D.P. Wilkinsona, S. Wessel, T.T. Cheng, J. Power Sources 205 (2012) 235–238.
[16] H. Li, S. Zhang, W. Qian, Y. Yu, X.-Z. Yuan, H. Wang, M. Jiang, S. Wessel, T.T. Cheng, J. Power Sources 218 (2012) 375–382.
[17] O.A. Baturina, A. Epshteyn, P.A. Northrup, K.E. Swider-Lyons, J. Electrochem. Soc. 158 (2011) B1198–B1205.
[18] T.J. Schmidt, U.A. Paulus, H.A. Gasteiger, R.J. Behm, J. Electroanal. Chem. 508 (2001) 41–47.
[19] G. Wu, Y.S. Chen, B.Q. Xu, Electrochem. Commun. 7 (2005) 1237–1243.
[20] G. Wu, B.Q. Xu, J. Power Sources 174 (2007) 148–158.
[21] E.S. Steigerwalt, G.A. Deluga, C.M. Lukehart, J. Phys. Chem. B 106 (2002) 760–766.
[22] M. Carmo, V.A. Paganin, J.M. Rosolen, E.R. Gonzalez, J. Power Sources 142 (2005) 169–176.
[23] J. Nakamura, in: T. Okado, M. Kaneko (Eds.), Molecular Catalysts for Energy Conversion, Springer Series in Materials Science, vol. 111, Springer-Verlag, Berlin Heidelberg, 2009, pp. 185–197.
[24] N. Muthuswamy, J.L.G. de la Fuente, P. Ocha, R. Giri, S. Raaen, S. Sunde, M. Rønning, D. Chen, Phys. Chem. Chem. Phys. 15 (2013) 3803–3813.
[25] M. Tsypkin, S.T. Briskeby, O.E. Kongstein, B.T. Børresen, R. Tunold, in: The 8th Frumkin Symposium: "Kinetics of Electrode Processes" (Russian Academy of Sciences, Moscow, 18.10.2005–22.10.2005), John Wiley & Sons, Hoboken and New Jersey, 2005, p. 165.
[26] I. Kvande, S.T. Briskeby, M. Tsypkin, M. Rønning, S. Sunde, R. Tunold, D. Chen, Top. Catal. 45 (2007) 81–85.
[27] T. Schmidt, H. Gasteiger, G. Stab, P. Urban, D. Kolb, R. Behm, J. Electrochem. Soc. 145 (1998) 2354–2358.
[28] U. Paulus, T. Schmidt, H. Gasteiger, R. Behm, J. Electroanal. Chem. 495 (2001) 134–145.
[29] A. Zolfaghari, B.E. Conway, G. Jerkiewicz, Electrochim. Acta 47 (2002) 1173–1187.
[30] K. Kinoshita, J. Electrochem. Soc. 137 (1990) 845–848.
[31] M.T.M. Koper, Nanoscale 3 (2011) 2054–2073.
[32] J.M. Feliú, E. Herrero, V. Climent, in: E. Santos, W. Schmickler (Eds.), Catalysis in Electrochemistry, John Wiley & Sons, Inc., 2011, pp. 127–163.
[33] K. Mayrhofer, B. Blizanac, M. Arenz, V. Stamenkovic, P. Ross, N. Markovic, J. Phys. Chem. B 109 (2005) 14433–14440.
[34] F. Maillard, M. Martin, F. Gloaguen, J. Leger, Electrochim. Acta 47 (2002) 3431–3440.
[35] F. Maillard, S. Pronkin, E.R. Savinova, in: M.T. Koper (Ed.), Fuel Cell Catalysis, John Wiley & Sons, Inc., 2009, pp. 507–566.
[36] M. Watanabe, H. Sei, P. Stonehart, J. Electroanal. Chem. 261 (1989) 375–387.
[37] H. Yang, S. Kumar, S. Zou, J. Electroanal. Chem. 688 (2013) 180–188.
[38] K. Morisawa, M. Ishida, S. Yae, Y. Nakato, Electrochim. Acta 44 (1999) 3725–3729.